

# Crystal Structures of Substrate and Inhibitor Complexes with AmpC $\beta$ -Lactamase: Possible Implications for Substrate-Assisted Catalysis

Alexandra Patera,<sup>†</sup> Larry C. Blaszcak,<sup>‡</sup> and Brian K. Shoichet<sup>\*,†</sup>

Contribution from the Department of Molecular Pharmacology & Biological Chemistry, Northwestern University, 303 East Chicago Avenue, Chicago, Illinois 60611-3008, and Infectious Diseases Research, Lilly Research Laboratories, Eli Lilly & Co., Lilly Corporate Center, Indianapolis, Indiana 46285

Received May 15, 2000

**Abstract:** Group I  $\beta$ -lactamases are major resistance determinants to  $\beta$ -lactam antibiotics. Despite intense study, the identity of the catalytic base, the direction of hydrolytic attack, and the functional difference between  $\beta$ -lactam substrates and  $\beta$ -lactam inhibitors remain controversial. To explore these questions, we determined the X-ray crystal structures of several representative  $\beta$ -lactams in their acyl–adduct complexes with the group I  $\beta$ -lactamase AmpC. A complex with the substrate loracarbef and a deacylation-deficient mutant enzyme reveals an ordered water molecule that is consistent with  $\beta$ -face attack of the catalytic water in group I  $\beta$ -lactamases. The ring nitrogen of the substrate is placed to hydrogen-bond with this water in the position it is thought to adopt in the deacylation transition state. In complexes with the inhibitors cloxacillin and moxalactam, conformational restrictions displace the equivalent ring nitrogens, sterically blocking the formation of the presumed deacylation transition-state structure. In conjunction with earlier studies, these acyl–enzyme structures suggest that both Tyr150 and the ring nitrogen of the substrate itself stabilize the hydrolytic transition state, and that  $\beta$ -lactam inhibitors of group I  $\beta$ -lactamases can act by physically blocking this activation.

## Introduction

$\beta$ -Lactamases are the major resistance mechanism to  $\beta$ -lactam antibiotics, such as the penicillins and the cephalosporins; bacteria that express these enzymes increasingly threaten public health.<sup>1,2</sup> Several families of these enzymes have evolved, the most widespread of which are the group I and group II serine  $\beta$ -lactamases.<sup>3</sup> Group I  $\beta$ -lactamases, like AmpC, are prevalent among Gram negative hospital pathogens and are responsible for bacterial resistance to a broad spectrum of  $\beta$ -lactam antibiotics. This has prompted intense mechanistic and structural investigation.<sup>4–13</sup>

The overall mechanism of group I  $\beta$ -lactamases is well accepted, closely resembling that of group II  $\beta$ -lactamases such

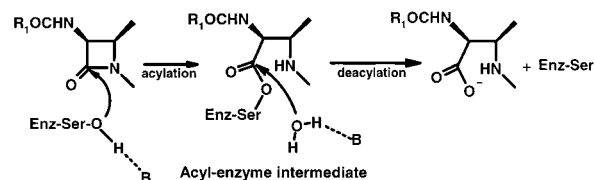


**Figure 1.** Simplified mechanism of  $\beta$ -lactam hydrolysis by group I  $\beta$ -lactamases. The  $\alpha$ -face of the  $\beta$ -lactam ring is below and the  $\beta$ -face is above the plane of the paper. For many  $\beta$ -lactams the second step is rate limiting in group I  $\beta$ -lactamases.

as TEM-1.<sup>8,10,14</sup> In the first step, the catalytic Ser64 attacks the lactam carbonyl carbon, opening the  $\beta$ -lactam ring to form an acylated enzyme intermediate. In the second step, this acyl intermediate is attacked by an activated water molecule, releasing the hydrolyzed  $\beta$ -lactam (Figure 1). For most  $\beta$ -lactams, deacylation is rate limiting.

Unlike the group II  $\beta$ -lactamases, the details of the rate-determining hydrolytic step remain controversial for the group I  $\beta$ -lactamases. Early structural studies suggested that the conserved Tyr150 was the catalytic base that activated the hydrolytic water for its attack on the acyl intermediate.<sup>8,14</sup> In the structure of a boronic acid transition-state analogue in complex with AmpC,<sup>13</sup> Tyr150 hydrogen-bonds with a hydroxyl of the tetrahedral center, consistent with its role as a catalytic base. Additionally, substitution of this residue by a Phe or a Ser reduces enzyme activity by as much as 10 000-fold.<sup>15</sup> However, other studies found that these substitutions affected catalysis only slightly for slowly hydrolyzed substrates, such

\* Corresponding author. E-mail: b-shoichet@northwestern.edu.

<sup>†</sup> Northwestern University.

<sup>‡</sup> Eli Lilly & Co.

(1) Neu, H. C. *Science* **1992**, 257, 1064–1073.

(2) Davies, J. *Science* **1994**, 264, 375–382.

(3) Bush, K.; Jacoby, G. A.; Medeiros, A. A. *Antimicrob. Agents Chemother.* **1995**, 39, 1211–1233.

(4) Tipper, D. J.; Strominger, J. L. *Proc. Natl. Acad. Sci. U.S.A.* **1965**, 54, 1133.

(5) Fisher, J.; Belasco, J. G.; Khosla, S.; Knowles, J. R. *Biochemistry* **1980**, 19, 2895–2901.

(6) Easton, C. J.; Knowles, J. R. *Biochemistry* **1982**, 21, 2857–62.

(7) Herzberg, O.; Moulton, J. *Science* **1987**, 236, 694–701.

(8) Oefner, C.; D'Arcy, A.; Daly, J. J.; Gubernatro, K.; Charnas, R. L.; Winkler, F. K. *Nature* **1990**, 343, 284–288.

(9) Strynadka, N. C. J.; Adachi, H.; Jensen, S. E.; Johns, K.; Sielecki, A.; Betzel, C.; Sutoh, K.; James, M. N. G. *Nature* **1992**, 359, 700–705.

(10) Lobkovsky, E.; Moews, P. C.; Liu, H.; Zhao, H.; Frere, J. M.; Knox, J. R. *Proc. Natl. Acad. Sci. U.S.A.* **1993**, 90, 11257–11261.

(11) Maveyraud, L.; Mourey, L.; Kotra, L. P.; Pedelacq, J. D.; Guillet, V.; Mobashery, S.; Samama, J. P. *J. Am. Chem. Soc.* **1998**, 120, 9748–9752.

(12) Usher, K.; Shoichet, B. K.; Blaszcak, L.; Weston, G. S.; Remington, J. R. *Biochemistry* **1998**, 37, 16082–16092.

(13) Powers, R. A.; Blazquez, J.; Weston, G. S.; Morosini, M. I.; Baquero, F.; Shoichet, B. K. *Protein Sci.* **1999**, 8, 2330–7.

(14) Lobkovsky, E.; Bilings, E. M.; Moews, P. C.; Rahil, J.; Pratt, R. F.; Knox, J. R. *Biochemistry* **1994**, 33, 6762–6772.

(15) Dubus, A.; Ledent, P.; Lamotte-Brasseur, J.; Frere, J. M. *Proteins* **1996**, 25, 473–485.

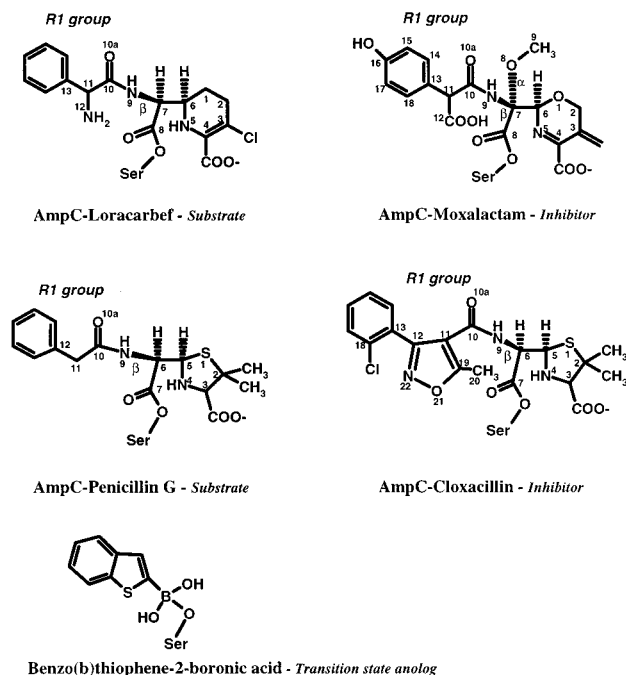


**Figure 2.** Characteristic  $\beta$ -lactam substrates and inhibitors of group I  $\beta$ -lactamases, and a transition-state analogue, in the enzyme-acylated form. The  $\alpha$ -face of the  $\beta$ -lactam ring is below and the  $\beta$ -face is above the plane of the paper. The R2 group of moxalactam has been eliminated owing to electronic rearrangement in the acyl adduct.<sup>40,41</sup>

as cefotaxime.<sup>16</sup> Furthermore, structural studies with other transition-state analogues<sup>12,14</sup> failed to reveal a direct role for Tyr150 in stabilizing the tetrahedral center. Studies of modified substrates<sup>17</sup> have suggested that the lactam ring nitrogen, and perhaps the exocyclic carboxylic acid of  $\beta$ -lactams themselves, act as the activating base in a substrate-assisted catalysis<sup>18</sup> mechanism.

The direction of hydrolytic attack also remains uncertain for group I  $\beta$ -lactamases. Structural considerations<sup>13,17</sup> suggest that the water attacks from the  $\beta$ -face of the lactam ring, in contrast to the case with the group II  $\beta$ -lactamases, where the water attacks from the  $\alpha$ -face<sup>9</sup> (Figure 1). However,  $\alpha$ -face-substituted  $\beta$ -lactams, such as moxalactam (Figure 2), which are thought to inhibit group II  $\beta$ -lactamases by displacing the catalytic water with bulky  $\alpha$ -face 6(7)-substituents,<sup>11</sup> also inhibit group I enzymes. It is unclear how a group on the  $\alpha$ -face of the ring would displace a water attacking from the other side.

Finally, the difference between a substrate  $\beta$ -lactam, such as penicillin, and an inhibitor  $\beta$ -lactam, such as cloxacillin, is often minor (Figure 2). Thus, penicillin and cloxacillin differ only in side chains that appear to be distant from the point of hydrolytic attack. How these differences distinguish substrate  $\beta$ -lactams, which are ineffective against AmpC-producing bacteria, from inhibitor  $\beta$ -lactams, which remain active against many such pathogens, is unclear.

In an effort to resolve these ambiguities, we have determined the crystal structures of three  $\beta$ -lactam acyl-enzyme complexes with AmpC from *Escherichia coli*. The structures of a substrate,

loracarbef,<sup>19</sup> and an inhibitor, cloxacillin<sup>20</sup> (Figure 2), were determined in complex with a deacylation deficient mutant AmpC, Q120L/Y150E. The structure of another inhibitor, moxalactam<sup>21</sup> (Figure 2), was determined in complex with wild-type (WT) AmpC. These structures suggest a mechanism that draws together earlier, seemingly incompatible results into a consistent picture for the rate-determining hydrolytic step in the mechanism of group I  $\beta$ -lactamases.

## Experimental Section

**Site-Directed Mutagenesis and Enzyme Preparation.** The Q120L/Y150E mutant of *E. coli* AmpC  $\beta$ -lactamase was made by oligonucleotide-directed mutagenesis.<sup>22</sup> The mutant enzyme was expressed as previously described.<sup>12</sup> To isolate the mutant protein, the growth medium supernatant was filtered, concentrated, dialyzed against 10 mM Tris-HCl (electrophoresis grade, FisherBiotech), pH 7.0, and passed over an S-Sepharose (Pharmacia) column equilibrated with dialysis buffer. The protein was eluted with a 10–100 mM Tris-HCl, pH 7.0, gradient. The protein elutes at 55 mM Tris-HCl. The protein appeared homogeneous by SDS-PAGE. The protein concentration was determined on the basis of absorbance at 280 nm, using an extinction coefficient of 2.4 OD (mg/mL)<sup>-1</sup> cm<sup>-1</sup>.<sup>12,23</sup>

**Crystal Growth.** Crystals of WT and Q120L/Y150E were grown by vapor diffusion in hanging drops over 1.7 M potassium phosphate buffer (pH 8.7) using microseeding techniques. The initial concentration of the protein in the drop was 100  $\mu$ M. Crystals appeared within 5–7 days after equilibration at 23 °C. For the cloxacillin structure, crystals of Q120L/Y150E were soaked in 30 mM cloxacillin in crystallizing buffer for another 30 min, and then soaked in 20% sucrose, 30 mM cloxacillin in crystallizing buffer for an additional 30 min before cryomounting. For the loracarbef/mutant and the moxalactam/AmpC complexes, crystals of enzyme were soaked in either 15 mM loracarbef or 50 mM moxalactam, respectively, in crystallizing buffer for 3 h, and then dipped in 20% sucrose, 15 mM loracarbef, or 50 mM moxalactam, respectively, in crystallizing buffer for 1 min. The crystals were frozen in liquid N<sub>2</sub> before cryomounting.

The crystallization buffer was prepared using ACS reagent grade potassium phosphate from Aldrich in deionized (MilliQ) 0.2- $\mu$ m filtered water. The  $\beta$ -lactam solutions were prepared by dissolving the  $\beta$ -lactam in crystallizing buffer or cryobuffer. Moxalactam and cloxacillin were purchased from Sigma-Aldrich, and loracarbef was a gift from Eli Lilly; all three were used without further purification.

**Data Collection and Processing.** The data were collected on an R-Axis-IIC image plate system at -144 °C for the loracarbef complex and at -167 °C for the cloxacillin and moxalactam complexes. For each of the three  $\beta$ -lactam/AmpC complexes, the data were collected from one crystal. The reflections were indexed, integrated, merged, and scaled using the Denzo/Scalepack program suite<sup>24</sup> (Table 1). The space group was C2, with two AmpC molecules in the asymmetric unit. In each complex, only poor electron density was observed for residues 280–291 of molecule 1, and five to six residues were left out of the refinement (Table 1). Molecule 2 of the asymmetric unit contained all 358 amino acids. Initial models were built using molecular replacement with the native structure.<sup>12</sup> Phases were calculated, and the models were subjected to rigid body, simulated annealing, and positional refinement techniques, all in CNS.<sup>25–27</sup> Electron density maps were calculated in CNS, and model building was done in the program O.<sup>28</sup> The ligands were built into the observed difference density, and the structures of the complexes were further refined in CNS.

(21) Mouton, R. P.; Bongaerts, G. P.; van Gestel, M.; Bruggeman-Ogle, K. M. *Chemotherapy* **1981**, 27, 318–24.

(22) Kunkel, T. A.; Roberts, J. D.; Zakour, R. A. *Methods Enzymol.* **1987**, 154, 367–382.

(23) Gill, S. C.; Hippel, P. H. v. *Anal. Biochem.* **1989**, 28, 319–326.

(24) Otwinowski, Z.; Minor, W. *Methods Enzymol.* **1997**, 276, 307–326.

(25) Brunger, A. T. *Nature* **1992**, 355, 472–5.

(26) Pannu, N. S.; Read, R. J. *Acta Crystallogr.* **1996**, A52, 659–668.

(27) Adams, P. D.; Pannu, N. S.; Read, R. J.; Brunger, A. T. *Proc. Natl. Acad. Sci. U.S.A.* **1997**, 94, 5018–23.

(28) Jones, T. A.; Zou, J. Y.; Cowan, S. W.; Kjeldgaard, M. *Acta Crystallogr.* **1991**, A47, 110–119.

(16) Dubus, A.; Normark, S.; Kania, M.; Page, M. G. *Biochemistry* **1994**, 33, 8577–8586.

(17) Bulychev, A.; Massova, I.; Miyashita, K.; Mobashery, S. *J. Am. Chem. Soc.* **1997**, 119, 7619–7625.

(18) Dall'Acqua, W.; Carter, P. *Protein Sci.* **2000**, 9, 1–9.

(19) Cao, C.; Chin, N. X.; Neu, H. C. *J. Antimicrob. Chemother.* **1988**, 22, 155–165.

(20) Knott-Hunziker, V.; Petursson, S.; SG, S. G. W.; Jaurin, B.; Grundstrom, T. *Biochem. J.* **1982**, 207, 315–322.

**Table 1.** Data Collection and Refinement Statistics

parameters	loracarbef/mutant	cloxacillin/mutant	moxalactam/WT
space group	C2	C2	C2
cell constants (Å, deg)	$a = 119.36, b = 76.26,$ $c = 98.36, \beta = 116.00$	$a = 118.52, b = 76.19,$ $c = 98.28, \beta = 116.68$	$a = 118.12, b = 77.16,$ $c = 97.92, \beta = 116.17$
resolution (Å)	2.35	2.46	2.20
unique reflections	33 137	26 662	39 390
$R_{\text{merge}}$ (%) <sup>a</sup>	8.1 (22.7)	12.1 (28.4)	11.4 (31.6)
completeness (%) <sup>a</sup>	95.0 (94.9)	92.8 (88.1)	98.0 (89.1)
$\langle I/\sigma_I \rangle$	11.9	12.4	12.8
resolution range for refinement (Å) <sup>a</sup>	8.0–2.35 (2.43–2.35)	20–2.46 (2.52–2.46)	8.0–2.20 (2.25–2.20)
number of protein residues	710	710	711
residues missing in monomer 1	Asn285–Lys290	Ile284–Asn289	Ser287–Ile291
number of non-hydrogen ligand atoms	52	62	62
number of water molecules	124	126	144
RMSD bond lengths (Å)	0.016	0.015	0.016
RMSD bond angles (deg)	1.9	1.9	1.8
$R_{\text{factor}}$ (%)	20.8	20.7	21.5
$R_{\text{free}}$ (%) <sup>b</sup>	25.8	26.5	25.9
average $B$ -factor, protein (Å <sup>2</sup> ) <sup>c</sup>	21.1	26.5	21.8
average ligand $B$ -factor (Å <sup>2</sup> ) <sup>c</sup>	35.7	41.2	33.9
% residues in most favored regions <sup>d</sup> (no Gly and Pro)	89.9	89.9	89.3
% residues in additionally allowed regions <sup>d</sup>	10.1	10.1	10.7

<sup>a</sup> Values in parentheses are for the highest resolution shell used in refinement. <sup>b</sup>  $R_{\text{free}}$  was calculated with 10% of reflections set aside randomly. <sup>c</sup> Values cited were calculated for both molecules in the asymmetric unit. <sup>d</sup> Ramachandran plot regions.

**Kinetics and Stability of Q120L/Y150E.** Enzyme assay conditions for AmpC have been previously described.<sup>29</sup> The values of  $k_{\text{cat}}$  and  $K_{\text{m}}$  for cephalothin were determined by monitoring reaction velocity while varying the cephalothin concentration, using a 20  $\mu\text{M}$  concentration of Q120L/Y150E in 50 mM phosphate buffer, pH 7.0, in 1-mm path length cells. Reversible thermal denaturation of Q120L/Y150E was performed in the absence and in the presence of cloxacillin, using circular dichroism to monitor the folded structure as previously described.<sup>30</sup>

**Fitting the Transition-State Analogue onto the Three  $\beta$ -Lactam/AmpC Structures.** Using the match command in MidasPlus,<sup>31</sup> the crystallographically determined structure of the transition-state analogue complex of BZBTH2B/AmpC<sup>13</sup> was fit onto the loracarbef/mutant, the cloxacillin/mutant, and the moxalactam/AmpC structures (see Figure 2 for compound structures). The C $\alpha$  atoms of residues 10–350 of molecule 2 were used to define the match.

A tetrahedral model of the substrate cephalothin, with its lactam bond opened and the attacking water covalently attached as a hydroxyl to the acyl carbon, was created using SYBYL (Tripos Assoc., St. Louis, MO). The R2 side chain was represented by an exocyclic methylene. Five hundred conformations for this molecule were calculated and docked into the site of the native enzyme<sup>12</sup> using the conformational ensemble version of the program DOCK.<sup>32</sup> A total of 6395 orientations of each of the conformations were calculated in the site. Each complex was scored on the basis of steric<sup>33</sup> and electrostatic complementarity, using a grid calculated by DelPhi.<sup>34,35</sup> The DIFDOCK option was used to bias the search to place the tetrahedral center in the active-site region, defined by atoms in a phosphate<sup>14</sup> and a boronic acid transition-state analogue complex.<sup>12</sup> To allow for covalent approach to Ser64, the C $\beta$  and O $\gamma$  atoms of this residue were deleted. The low-energy docking that had good distances to the Ser64 and the backbone nitrogens of Ser64 and Ala318 was RMS-fit onto the  $\beta$ -lactam/enzyme structures, as above.

(29) Weston, G. S.; Blazquez, J.; Baquero, F.; Shoichet, B. K. *J. Med. Chem.* **1998**, *41*, 4577–4586.

(30) Beadle, B. M.; McGovern, S. L.; Patera, A.; Shoichet, B. K. *Protein Sci.* **1999**, *8*, 1816–24.

(31) Ferrin, T. E.; Huang, C. C.; Jarvis, L. E.; Langridge, R. *J. Mol. Graph.* **1988**, *6*, 13–27.

(32) Lorber, D. M.; Shoichet, B. K. *Protein Sci.* **1998**, *7*, 938–950.

(33) Shoichet, B.; Bodian, D. L.; Kuntz, I. D. *J. Comput. Chem.* **1992**, *13*, 380–397.

(34) Gilson, M. K.; Honig, B. H. *Nature* **1987**, *330*, 84–86.

(35) Meng, E. C.; Shoichet, B.; Kuntz, I. D. *J. Comput. Chem.* **1992**, *13*, 505–524.

(36) Laskowski, R. A.; MacArthur, M. W.; Moss, D. S.; Thornton, J. M. *J. Appl. Crystallogr.* **1993**, *26*, 283–291.

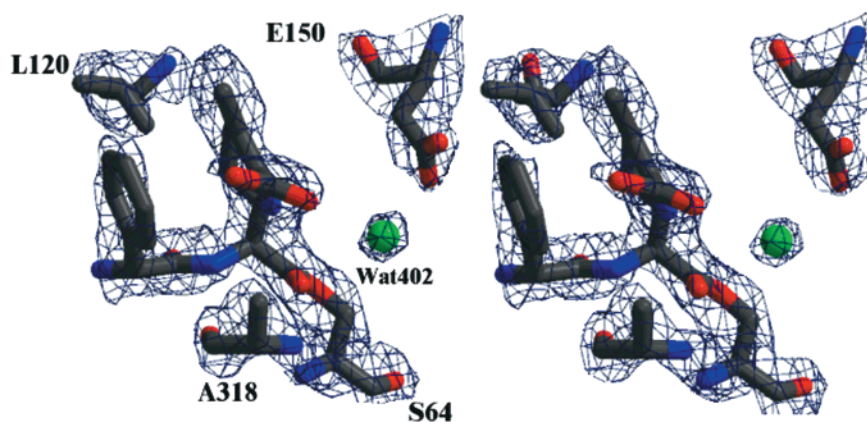
## Results

In an effort to capture a substrate–enzyme complex, the mutant enzyme Q120L/Y150E was made by site-directed mutagenesis. A substitution at Tyr150 seemed sensible, given its proposed role as the catalytic base in deacylation of  $\beta$ -lactam–AmpC adducts; a functionally related mutant of TEM-1  $\beta$ -lactamase (E166N) had been used to determine the structure of an acyl–enzyme complex of that enzyme.<sup>9</sup> Also, the substitution of Tyr150  $\rightarrow$  Glu might be expected to preserve interactions with a putative hydrolytic water (such interactions are, in fact, observed in the loracarbef structure, see below). The Q120L/Y150E mutant enzyme was 20 000-fold less active than the native enzyme, based on its ability to hydrolyze the characteristic substrate cephalothin. Thermal denaturation<sup>30</sup> of Q120L/Y150E in the presence of cloxacillin indicated that this mutant rapidly forms a covalent acyl adduct (unpublished data). These results suggest that the mutant enzyme is deacylation deficient, consistent with earlier work.<sup>15</sup>

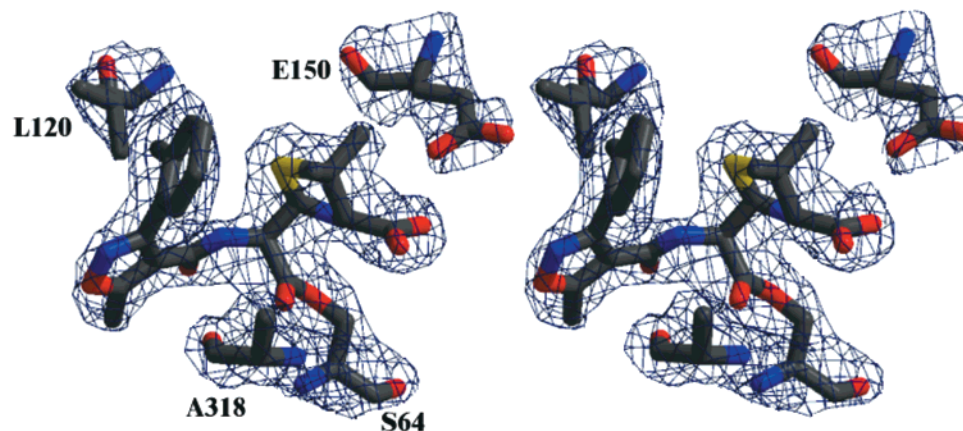
The X-ray crystallographic structures of loracarbef, cloxacillin, and moxalactam complexed with either Q120L/Y150E or WT were determined to 2.35, 2.46, and 2.20 Å resolution, with  $R/R_{\text{free}}$  values of 20.8%/25.8%, 20.7%/26.5%, and 21.5%/25.9%, respectively (Table 1). All residues are in allowed regions of the Ramachandran plot, as evaluated by Procheck<sup>36</sup> (Table 1). Following refinement, simulated annealing omit maps of the ligand region were calculated and showed unambiguous, connected positive difference density for the compounds when contoured at  $3\sigma$ . In each structure, the electron density for the  $\beta$ -lactam was well defined (Figure 3).

For each complex, the crystallographic space group was C2, with two molecules in the asymmetric unit. In the descriptions that follow, we will focus on molecule 2 of the asymmetric unit, which had better density and temperature factors than molecule 1 in all three structures. All 358 amino acids were modeled for molecule 2 of the asymmetric unit for each complex, whereas only partial electron density was observed for residues 280–291 of molecule 1, and five or six residues were left out of the refinement of this molecule (Table 1). In molecule 2, the ligand temperature factors for the loracarbef, cloxacillin, and moxalactam complexes were in the 20–30 Å<sup>2</sup> range in the ring portions of the ligands, which are most closely

a.



b.



c.

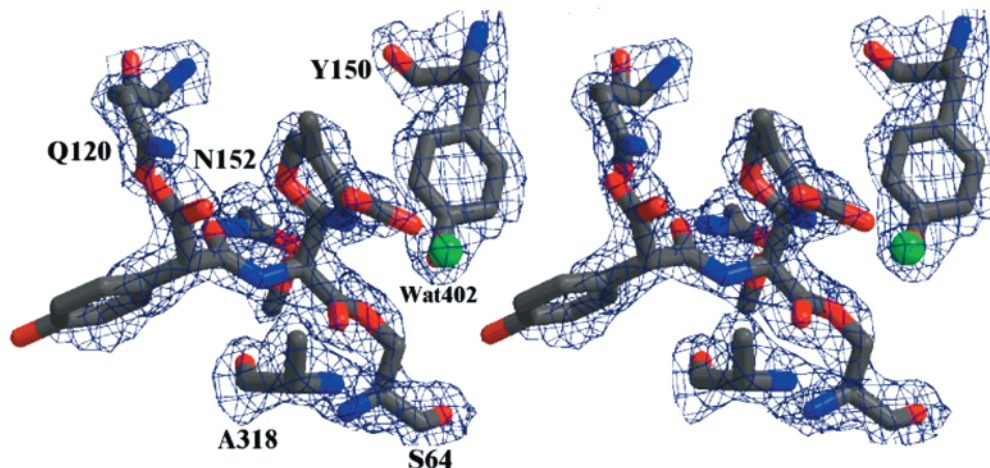


**Figure 3.** Stereoview of  $2F_o - F_c$  electron density of the refined models for complexes of loracarbef/mutant, cloxacillin/mutant, and moxalactam/AmpC contoured at  $1\sigma$ . All of the figures show the same active-site region, from the same perspective, of the enzyme- $\beta$ -lactam adduct. (a) The substrate loracarbef covalently bound to Q120L/Y150E. (b) The inhibitor cloxacillin bound to Q120L/Y150E. (c) The inhibitor moxalactam bound to WT AmpC. In all the figures, carbon atoms are colored gray, oxygen atoms red, and nitrogen atoms blue. The green sphere in (a) and (c) represents the putative deacylating water molecule. These figures were generated using the programs MolScript<sup>42</sup> and Raster 3D<sup>43</sup> and displayed using Bobscrip<sup>44</sup>.

involved with the key catalytic residues. For the cloxacillin and loracarbef complexes, there are no significant differences in the placement of the  $\beta$ -lactam rings between the two molecules in the asymmetric unit. In the moxalactam complex, the oxacephem ring of moxalactam has rotated by almost  $180^\circ$  about the C6-C7 bond (Figure 2) in molecule 1 compared to molecule 2 of

the asymmetric unit. This rotation places the oxacephem ring oxygen in the position occupied by the ring nitrogen in molecule 2. This does not affect the conclusions that we will draw from this structure, which relate to steric occlusion by the oxacephem ring (see below).

**Interactions Common to All Three Complexes.** The

**Table 2.** Interaction Distances between the  $\beta$ -Lactam Core of the Ligands and AmpC Residues

interactions	distance ( $\text{\AA}$ ) <sup>a</sup>			
	loracarbef/utant	cloxacillin/mutant	moxalactam/WT	apo-WT
Y150OH/Wat500 <sup>b</sup> -S64O $\gamma$	3.1	n.o. <sup>c</sup> (3.7)	2.8	3.2
Y150OH/Wat500 <sup>b</sup> -K67N $\zeta$	3.0	2.5	2.8	3.1
Y150OH/Wat500 <sup>b</sup> -K315N $\zeta$	3.1	3.4	2.9	2.6
Glu150O $\epsilon$ -Wat500	2.6	2.6	n.o. <sup>c</sup>	n.o. <sup>c</sup>
T316O-K315N $\zeta$	3.0	2.9	3.2	3.2
N152O $\delta$ 1-K67N $\zeta$	3.1	2.9	2.8	2.7
N152O $\delta$ 1-Q120O $\epsilon$ 1(L120C $\delta$ 2) <sup>d</sup>	n.o. <sup>c</sup> (3.5)	n.o. <sup>c</sup> (3.6)	3.0	3.1
$\beta$ -lactam O-A318N	3.1	3.2	3.0	
$\beta$ -lactam O-A318O	3.5	3.2	3.3	
$\beta$ -lactam O-S64N	3.1	3.0	2.9	
$\beta$ -lactam R <sub>1</sub> O-N152N $\delta$ 2	2.7	2.6	3.3	
$\beta$ -lactam R <sub>1</sub> N9-A318O	3.1	n.o. <sup>c</sup> (4.0)	3.2	
$\beta$ -lactam R <sub>1</sub> O-Q120N $\epsilon$ 2	n.o. <sup>c</sup>	n.o. <sup>c</sup>	3.0	
Wat402-T316O $\gamma$	3.1		3.2	n.o. <sup>c</sup> (3.9 <sup>e</sup> )
Wat402- $\beta$ lactam C7(8)	4.0		3.7	
Wat402- $\beta$ -lactam C3(C4)COOH O1	n.o. <sup>c</sup> (3.3)		2.7	
Wat402- $\beta$ -lactam N4(5)	n.o. <sup>c</sup> (3.6)		3.0	
Wat402-Wat403	2.8			
BZBTH2B O2- $\beta$ -lactam N4(5)	2.4	0.9	1.6	
N289N $\delta$ 2- $\beta$ -lactam C3 (C4)COOH O2	n.o. <sup>c</sup> (4.0)	n.o. <sup>c</sup> (5.8)	3.2	
N346N $\delta$ 2- $\beta$ -lactam C3(C4)COOH O1	n.o. <sup>c</sup> (3.9)	n.o. <sup>c</sup>	3.2	
N346N $\delta$ 2- $\beta$ -lactam C3(C4)COOH O2	n.o. <sup>c</sup>	3.1	n.o. <sup>b</sup>	
$\beta$ -lactam C3(C4)COOH O1-Wat401	2.7	n.o. <sup>c</sup>	2.6	
$\beta$ -lactam C3(C4)COOH)1-Wat400	2.9	-	n.o. <sup>c</sup>	
$\beta$ -lactam C3(C4)COOH O2-Wat401	n.o. <sup>c</sup>	2.8	3.1	
$\beta$ -lactam C3(C4)COOH O2-Wat400	2.7		2.8	
$\beta$ -lactam C3(C4)COOH O2-Wat406			2.8	

<sup>a</sup> All distances are for molecule 2 of the asymmetric unit. <sup>b</sup> Tyr150 in the native structures, Wat500 in the mutant structures. <sup>c</sup> Interaction is not observed. <sup>d</sup> Residue 120 is either Q or L, depending on whether wild-type or mutant complex, respectively. <sup>e</sup> Wat402 is equivalent to Wat387 in native structure.<sup>12</sup>

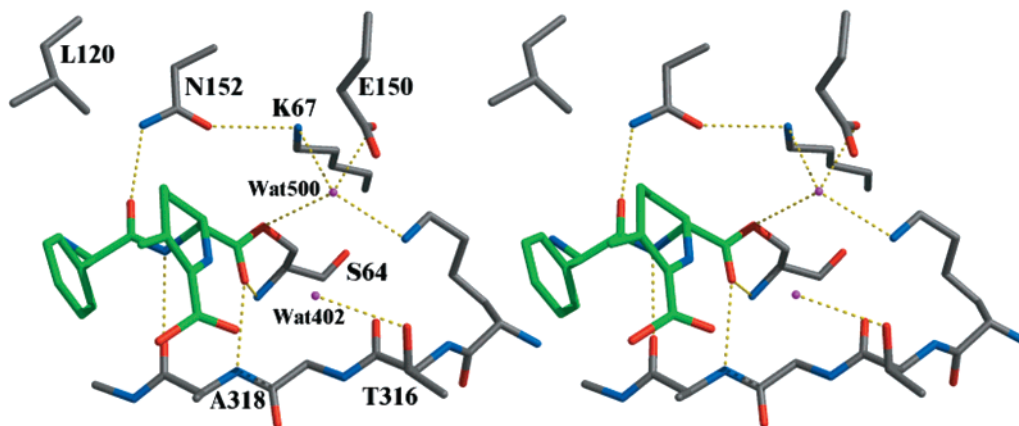


**Figure 4.** Key polar interactions observed in the structure of loracarbef in complex with Q120L/Y150E. Dashed lines indicate hydrogen bonds; the purple spheres represent water molecules. Wat402 is the putative deacylating water molecule. Atoms are colored as in Figure 3. Loracarbef carbons are green. Interaction distances are listed in Table 2. Figures 4–7 were made with MidasPlus.<sup>45</sup>

conformation of AmpC in the loracarbef, cloxacillin, and moxalactam complexes resembles that of the apo-enzyme, with an RMSD from the  $\alpha$  carbon atom positions of the apo structure of 0.48, 0.46, and 0.57  $\text{\AA}$ , respectively. All three of the  $\beta$ -lactams make several anticipated interactions (Table 2), based on previous structural studies. These include hydrogen bonds between the  $\beta$ -lactam carbonyl oxygen and both Ser64N and Ala318N, which are thought to activate the carbonyl for hydrolytic attack.<sup>8,9,14,37</sup> The amide portion of the R1 side chain (Figure 2) of all three  $\beta$ -lactams fits into a region lined by the conserved residues Asn152, Ala318, and Gln120 (Leu120 in Q120L/Y150E). In each complex, the amide oxygen hydrogen-bonds with Asn152N $\epsilon$ 2 (Figures 4–6). In the loracarbef and moxalactam structures, the amide nitrogen also hydrogen-bonds

to the main-chain oxygen of Ala318; in the cloxacillin structure this interaction is not observed. In the Q120L/Y150E complexes, the side chain of Leu120 does not interact directly with the ligands. In the WT AmpC complex, a hydrogen bond is observed between Gln120N $\epsilon$ 2 and the R1 side chain carbonyl oxygen of moxalactam. Few interactions are observed beyond the amide functionality of the R1 side chain. In the loracarbef complex, the N12 of the R1 side chain hydrogen-bonds with two ordered water molecules. In the moxalactam complex, the R1 phenolic hydroxyl hydrogen-bonds with an ordered water, as does the R1 carboxylic acid.

**The Loracarbef Complex.** A key observation in the complex between the substrate loracarbef and the mutant enzyme is the presence of a well-ordered water molecule ( $B$ -factor = 20.0  $\text{\AA}^2$ ) near the hydrolytic center (Figure 4). The water, Wat402, is

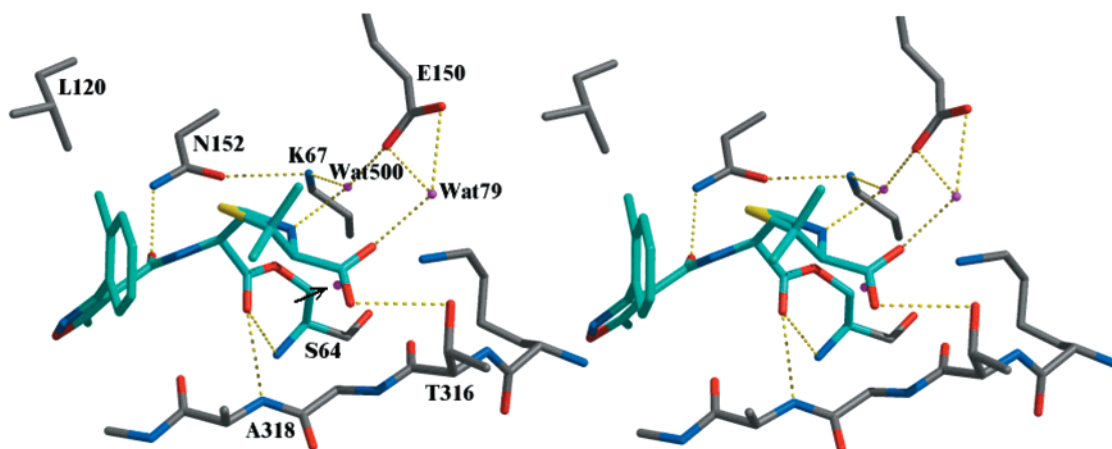


**Figure 5.** Key polar interactions observed in the structure of cloxacillin in complex with the mutant enzyme. Dashed lines indicate hydrogen bonds. The purple sphere indicated by the arrow represents the putative deacylating water molecule that is present in the substrate complex (Figure 4) but absent in this inhibitor complex. Atoms are colored as in Figure 3. Cloxacillin carbons are in cyan. Interaction distances are listed in Table 2.

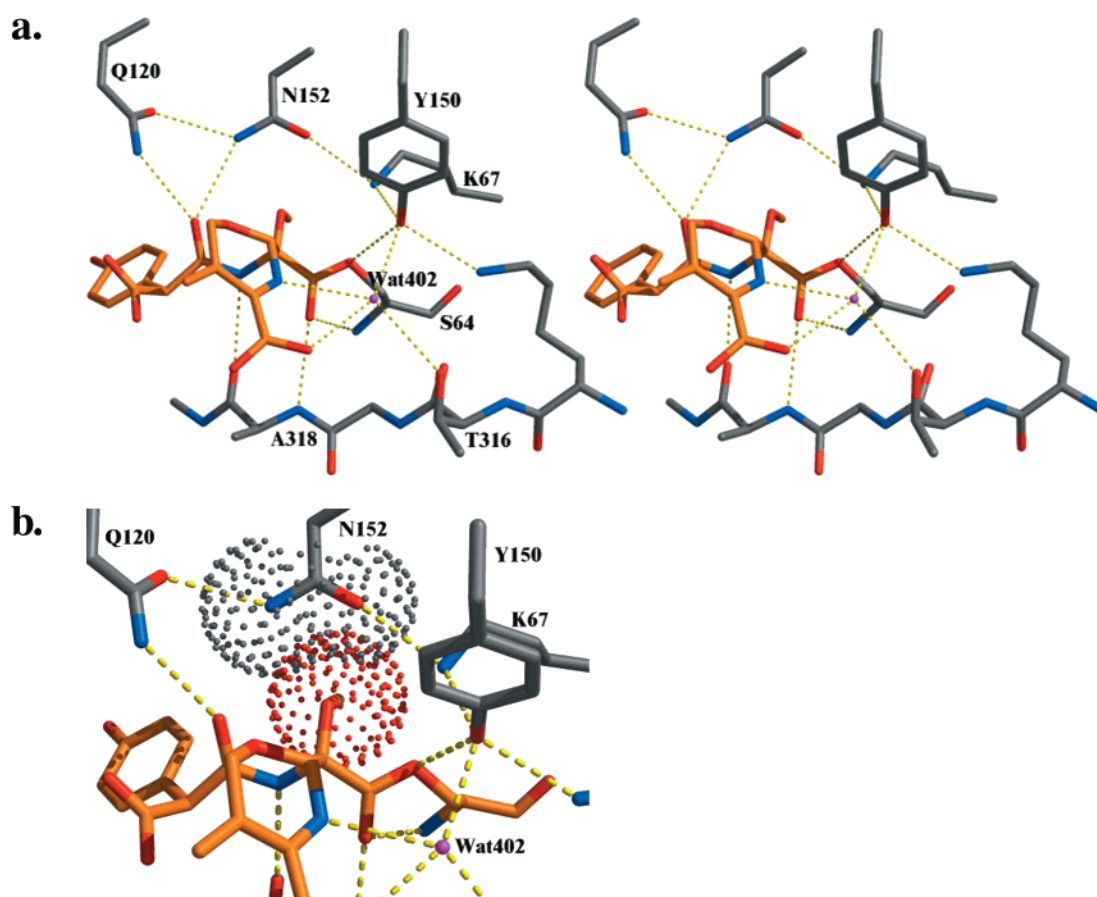


**Figure 6.** (a) Key polar interactions observed in the structure of moxalactam in complex with wild-type AmpC. Dashed lines indicate hydrogen bonds. Atoms are colored as in Figure 3. Moxalactam carbons are orange. Interaction distances are listed in Table 2. (b) Close-up of view of van der Waals overlaps between Asn152 and the  $7\alpha$ -methoxy group of moxalactam (Figure 2).

located on what was the  $\beta$ -face of the now open lactam ring of loracarbef, forming hydrogen bonds to Thr316O $\gamma$ , Wat403 (not shown in Figure 4), and possibly the C4 carboxylate of the carbacephem ring (distance 3.3 Å). It is 4.0 Å away from the carbonyl carbon of the acyl-enzyme complex and appears to have an unobstructed line of attack to the acyl center. The position of Wat402 is highly conserved in the structures of group I  $\beta$ -lactamases. Wat402 is 1.1 Å from Wat226 in the structure

of the group I  $\beta$ -lactamase from *E. cloacae* (PDB 1BLS),<sup>14</sup> 0.7 Å from Wat387 in the AmpC native structure (PDB 2BLS),<sup>12</sup> and 0.3 Å from Wat402 in the structure of a transition-state analogue, benzo[*b*]thiophene-2-boronic acid (BZBTH2B), in complex with AmpC (PDB 1C3B).<sup>13</sup>

We compared the loracarbef acyl complex to its likely tetrahedral high-energy intermediate structure. This structure was surmised from the crystal structure of the transition-state

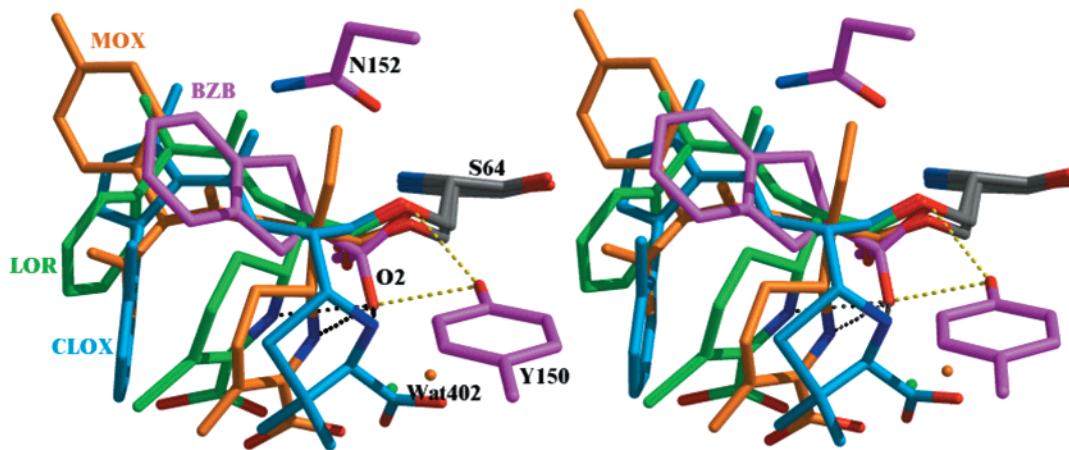


**Figure 7.** Overlay of the three  $\beta$ -lactam complexes and the tetrahedral transition-state analogue, BZBTH2B. Loracarbef, cloxacillin, moxalactam, and BZBTH2B are colored green, cyan, orange, and magenta, respectively. Carbon atoms of residues Asn152 and Tyr150 from the BZBTH2B/AmpC complex<sup>13</sup> are colored magenta. The distances between the O2 of BZBTH2B, presumed to represent the deacylating water in the transition state, and the N4(5), colored blue, of the  $\beta$ -lactams are 2.4, 0.9, and 1.6 Å for loracarbef, cloxacillin, and moxalactam, respectively (black lines). The yellow dashed lines indicate hydrogen bonds observed in the BZBTH2B/AmpC complex. The green and orange spheres represent the deacylating water, Wat402, in the loracarbef/mutant and moxalactam/AmpC complexes, respectively.

analogue BZBTH2B in complex with AmpC, and also from a docked model of a cephalosporin in its tetrahedral high-energy intermediate conformation with AmpC. The RMSD<sub>C $\alpha$</sub>  of the BZBTH2B/AmpC and the loracarbef/mutant structure is 0.30 Å (Figure 7). In this superposition, the O2 of the boronic acid, thought to represent the position of the deacylating water in the transition state,<sup>13</sup> is 2.4 Å from the carbacephem ring N5 of the loracarbef. The O2 of the boronic acid is located approximately perpendicular to the plane formed by the double bond in the substrate ring (Figure 2), at an angle of 108° to the ring plane. This angle might suggest that the O2 hydroxyl of the boronic acid is interacting with the nitrogen lone pair, which should be localized perpendicular to the ring plane. The angle between the boron, O2, and substrate nitrogen is 84°—ideally, one would expect this angle to be closer to 109°. Nevertheless, if this ring nitrogen could occupy a similar position in the transition state, it would be well placed to hydrogen-bond with the hydrolytic water as it attacks the acyl center.

Similar observations are made when we fit a tetrahedral model of the characteristic substrate cephalothin into AmpC, using a multiconformational version of the docking program DOCK.<sup>32</sup> This model of the tetrahedral high-energy intermediate resembles that of crystallographic loracarbef/mutant structure, with the exception that the planar acyl center in loracarbef has been modeled as tetrahedral in the cephalothin model. The distance from the cephalothin N5 to its own O2 oxygen, representing the deacylating water, is 2.3 Å; the distance from the loracarbef N5 nitrogen to this oxygen position would be 2.5 Å. This suggests that the putative hydrogen-bond between the ring nitrogen and the oxygen of the tetrahedral intermediate is not peculiar to the boronic acid or to loracarbef. In both the crystallographic transition-state analogue complex and the modeled cephalothin tetrahedral intermediate complex, the Tyr150OH hydrogen-bonds to the same tetrahedral oxygen as does the ring nitrogen of the substrate (see Figure 7, below).

The substituted Glu150 occupies a position similar to that of Tyr150 in native structures,<sup>13,12</sup> except that the shorter glutamate cannot extend to replace the hydroxyl of the tyrosine. Instead, Glu150 hydrogen-bonds with an ordered water, Wat500, which is 0.3 Å from the position occupied by the Tyr150OH in the native structures (Figure 4). Wat500 hydrogen-bonds with the same residues with which the Tyr150OH normally interacts: Lys67N $\zeta$ , Lys312N $\zeta$ , and Ser64O $\gamma$ . These conserved interac-

tions speak to the functional importance of the tyrosine hydroxyl; its replacement by a water, which would be less active in acid–base catalysis, may explain much of the decreased activity of this mutant AmpC.

Finally, the exocyclic C4 COOH group of the loracarbef carbacephem ring hydrogen-bonds with two ordered waters, Wat401 and Wat400 (not shown in Figure 4). Wat401, in turn, is coordinated to Arg349NH1, Asn346O $\delta$ 1, and Gly317O. Wat400 interacts with Asn343N $\delta$ 2 and Asn343O $\delta$ 1. The carboxylate may form a long hydrogen bond with the putative deacylating Wat402 (a distance of 3.3 Å). The locations of this carboxylate and the ring to which it is attached differ considerably from their locations in the cloxacillin and moxalactam complexes (see Figures 5 and 6, below).

**The Cloxacillin Complex.** A key difference between the cloxacillin/mutant and the loracarbef/mutant complexes is the placement of the penicillanic ring of cloxacillin compared to the analogous carbacephem ring of loracarbef. The R1 side chain of cloxacillin contains a bulky phenyl-isoxazole group. In two dimensions (Figure 2), this group appears to be distant from the point of chemical attack in  $\beta$ -lactams. In three dimensions, this group folds back, like a scorpion's tail, toward the penicillanic ring (Figures 5 and 7). This appears to induce a  $-58^\circ$  rotation of the penicillanic ring of the inhibitor about its C5–C6 bond (Figure 2), compared to the conformation adopted by loracarbef. Without this rotation, the penicillanic methyl would have been 2.2 Å from the phenyl-isoxazole, in violation of van der Waals limits. This rotation places the C3 COOH of the penicillanic ring in the site of Wat402 in the loracarbef complex, displacing this water (Figure 5).

As in the loracarbef complex, Wat500 has replaced the Tyr150OH, forming hydrogen bonds with the substituted Glu150O $\epsilon$ 1, Lys67N $\zeta$ , and Lys315N $\zeta$ . The rotated position of the penicillanic acid ring of cloxacillin displaces Wat500 somewhat, so that its distance to the position formerly occupied by the tyrosine hydroxyl is 0.7 Å. The Glu150 has swung out of the position adopted in the loracarbef structure, also reflecting the crowding by the penicillanic acid ring of the inhibitor.

We again overlaid the cloxacillin acyl adduct onto deacylation tetrahedral intermediate structures inferred from the crystallographic structure of BZBTH2B/AmpC and from a model of a tetrahedral conformation of cephalothin/AmpC. The transition-state analogue complex was fit to the cloxacillin complex

(RMSD<sub>C $\alpha$</sub>  = 0.30 Å, Figure 7). In the resulting overlay, the tetrahedral O2 of the transition-state analogue is 0.9 Å from the cloxacillin penicillanic N4. A similar distance to the equivalent oxygen is observed in the docked model of a tetrahedral conformation of cephalothin in AmpC. This distance is so close as to block the formation of the tetrahedral high-energy intermediate.

**The Moxalactam Complex.** The inhibitor moxalactam was determined in complex with WT AmpC. As in the cloxacillin complex, the placement of the oxacephem ring in the inhibitor moxalactam complex differs from that of the analogous carba-cephem ring of the substrate loracarbef (Figure 6a). The 7 $\alpha$ -methoxy group of moxalactam (Figure 2) is within 2.9 Å of Asn152O $\delta$ 1; this unfavorable contact (Figure 6b) leads to a  $-25^\circ$  rotation about the moxalactam C7–C8 bond, compared to the conformation adopted by loracarbef. This relieves what would have been severe steric violations involving the 7 $\alpha$ -methoxy and Asn152, but it also displaces the oxacephem ring so that the C4 COOH group has moved by 1.9 Å relative to that in the loracarbef structure. This movement, in turn, displaces the putative deacylating water, Wat402, by 1.2 Å compared to the loracarbef structure, though it remains on the  $\beta$ -face of the opened  $\beta$ -lactam ring. In its new position, Wat402 is coordinated by four groups: the oxacephem N5 and the C4 COOH from the inhibitor, and the Tyr150OH and the Thr316O $\gamma$  from the enzyme (Table 2). This may be compared to the loracarbef structure, where Wat402 makes only two hydrogen bonds, one of which is to another water.

As with the cloxacillin structure, a key feature of the moxalactam complex appears to be steric occlusion of the yet-to-be-formed tetrahedral high-energy intermediate. When the structure of the transition-state analogue complex, BZBTH2B/AmpC, is overlaid on the moxalactam/AmpC structure (RMS<sub>C $\alpha$</sub>  = 0.25 Å, Figure 7), the moxalactam oxacephem ring N5 (Figure 2) is 1.6 Å from the O2, representing the incoming deacylating water of the transition-state analogue. The same distance is observed in the model of the tetrahedral cephalothin/AmpC. This short distance would be expected to block formation of the high-energy intermediate.

In this WT AmpC complex, Tyr150 is in the same position as in earlier native structures. We note that the hydroxyl of Tyr150 is within 2.9 Å of four potential hydrogen-bonding partners: Lys67N $\zeta$ , Lys315N $\zeta$ , Wat402, and Ser64O $\gamma$ . The geometry is consistent with a bifurcated hydrogen bond from Tyr150OH to Wat402 and Ser64O $\gamma$ .<sup>38</sup>

## Discussion

A key to understanding these acyl–enzyme complexes comes from their comparison to structures representing the deacylation tetrahedral high-energy intermediate for the AmpC reaction. In the loracarbef complex, the ring nitrogen of the substrate is placed such that in the high-energy intermediate it would be 2.4 Å from the tetrahedral oxygen representing the hydrolytic water. In an overlay of the loracarbef/mutant complex with a transition-state analogue complex,<sup>13</sup> both the substrate ring nitrogen and the hydroxyl of Tyr150 hydrogen-bond with the O2 representing the hydrolytic water (Figure 7). This would explain why both groups are necessary for rapid deacylation of  $\beta$ -lactams. At the same time it suggests how the loss of one of these two groups dramatically reduces, but does not abolish, catalysis. Especially for slow substrates,<sup>15</sup> the loss of one of these groups may be partly compensated by the presence of

the other. The hydrogen bond between Tyr150 and the O2 oxygen is consistent with a role for Tyr150 as a catalytic base,<sup>14,15</sup> especially if the residue were present as a tyrosinate (the protonation state of this residue is unknown to us). The role of the ring nitrogen of loracarbef in stabilizing its own deacylation high-energy intermediate is consistent with a substrate-assisted mechanism of catalysis, as suggested by Mobashery and colleagues.<sup>17</sup>

The complexes of the inhibitors, cloxacillin and moxalactam, with AmpC are consistent with this mechanism. Whereas in the loracarbef structure the ring nitrogen is poised to stabilize the tetrahedral high-energy intermediate, in the inhibitor structures the equivalent nitrogens occupy positions that block the formation of this intermediate (Figure 7). In the cloxacillin complex, the conformationally restricted side chain of the inhibitor folds back on the penicillanic acid ring, displacing it. This places the ring nitrogen 0.9 Å from where a tetrahedral oxygen of the high-energy intermediate would be expected to exist in a substrate structure. In the moxalactam complex, the  $\alpha$ -face methoxy group sterically conflicts with the conserved Asn152, forcing accommodations that displace the oxacephem ring. This places the ring nitrogen 1.6 Å from where the tetrahedral oxygen would be placed in the presumptive transition state. Unlike group II  $\beta$ -lactamases, where the water attacks from the  $\alpha$ -face of the substrate, in group I  $\beta$ -lactamases,  $\alpha$ -face inhibitors, such as moxalactam, do not displace the hydrolytic water directly, but rather appear to destabilize the tetrahedral high-energy intermediate by forcing the activating ring nitrogen out of position.

Surprisingly, cloxacillin and moxalactam, which are less similar to each other than each is to several substrate  $\beta$ -lactams (Figure 2), both act as inhibitors owing to steric obstructions that displace the key ring nitrogen in the active site (Figure 7). In the case of cloxacillin, this steric occlusion is internal to the inhibitor, whereas in moxalactam it occurs between the inhibitor and the enzyme. This is consistent with thermal denaturation studies that show that cloxacillin stabilizes AmpC on binding, whereas moxalactam destabilizes the enzyme.<sup>30</sup>  $\beta$ -Lactam inhibitors that differ considerably from each other may, nonetheless, inhibit group I  $\beta$ -lactamases in the same manner, namely by destabilizing the formation of the deacylation transition state.

A caveat to this model of substrate-assisted catalysis and its inhibition is that it does not explain the ability of group I  $\beta$ -lactamases to hydrolyze depsipeptides. Several of these are good substrates for these enzymes,<sup>39</sup> despite the fact that they do not contain an equivalent of the lactam nitrogen proposed here to participate in stabilizing the tetrahedral high-energy intermediate. Depsipeptides may rely exclusively on Tyr150 to stabilize the hydrolytic water in the high-energy intermediate. By extension, an alternate model for  $\beta$ -lactam hydrolysis would be one where Tyr150 alone is responsible for stabilizing the high-energy tetrahedral intermediate, with the proximity of the lactam nitrogen of the substrate being largely epiphenomenal. In this model, the inhibition of cloxacillin and moxalactam might derive from their displacement of the proposed hydrolytic Wat402, and not from their blocking the formation of the tetrahedral high-energy intermediate as proposed above. We certainly cannot discount this alternative model, but we do not favor it. Although the putative deacylating Wat402 has been completely displaced in the cloxacillin/mutant structure, this water is moved by only 1.2 Å in the moxalactam/AmpC

(38) Preissner, R.; Egner, U.; Saenger, W. *FEBS Lett* **1991**, *288*, 192–196.

(39) Xu, Y.; Soto, G.; Hirsch, K. R.; Pratt, R. F. *Biochemistry* **1996**, *35*, 3595–3603.

structure, suggesting it is still available to attack the acyl intermediate. Additionally, this alternative model does not seem to explain  $\beta$ -lactam modification studies<sup>17</sup> that suggest that the lactam nitrogen participates in the catalytic mechanism. Distinguishing between these two views conclusively may await further studies.

**A Model for the Deacylation Mechanism of Group I  $\beta$ -Lactamases.** We present a model that seems most consistent with previous mutagenesis, substrate modification, and structural data on the deacylation mechanism of  $\beta$ -lactams by group I  $\beta$ -lactamases. In the acyl intermediate,  $\beta$ -lactam substrates are oriented in the active site by multiple interactions in a conformation similar to that adopted by loracarbef. Water attacks this intermediate from its  $\beta$ -face, from what appears to be a structurally conserved position represented by Wat402 in the loracarbef/mutant complex. As the hydrolytic water attacks the acyl intermediate, i.e., in the high-energy intermediate, it moves to a position where it is stabilized by interactions with both the

oxygen of Tyr150 and the ring nitrogen of the substrate itself. If Tyr150 were present as the tyrosinate, it would be well placed to play the role of the catalytic base. Subsequently, as observed in the phosphonate/P99 complex from *E. cloacae*,<sup>14</sup> the hydroxyl of Tyr150 switches to activating the O $\gamma$  of Ser64 for departure from the acyl adduct. The switching of Tyr150 from the attacking water to the leaving group Ser64 may represent the two deacylation transition states that have been proposed for group I  $\beta$ -lactamases.<sup>14</sup> The ability to displace their own functionality, the catalytically important ring nitrogen of  $\beta$ -lactams, seems to distinguish  $\beta$ -lactam inhibitors from  $\beta$ -lactam substrates, and consequently  $\beta$ -lactams that are active against AmpC-expressing bacteria from  $\beta$ -lactams to which these pathogens are resistant.

**Coordinates.** The coordinates for loracarbef/Q120L/Y150E, cloxacillin/Q120L/Y150E and moxalactam/AmpC have been deposited in the Protein Data Bank (accession codes are 1FCN, 1FCM, and 1FCO, respectively).

**Acknowledgment.** This work was supported by grants NSF MCB9734484 and NIH GM59957 (to B.K.S.). We thank B. Beadle, D. Freymann, S. Garman, S. McGovern, and R. Powers for reading this manuscript. We thank D. Freymann and P. Focia for crystallographic advice.

JA001676X

(40) Nishikawa, J.; Watanabe, F.; Shudou, M.; Terui, Y.; Narisada, M. *J. Med. Chem.* **1987**, *30*, 523–527.

(41) Kuzin, A. P.; Liu, H.; Kelly, J. A.; Knox, J. R. *Biochemistry* **1995**, *34*, 9532–9540.

(42) Kraulis, P. J. *J. Appl. Crystallogr.* **1991**, *24*, 946–950.

(43) Bacon, D. J.; Anderson, W. F. *J. Mol. Graph.* **1988**, *6*, 210–220.

(44) Esnouf, R. H. *J. Mol. Graph. Model* **1997**, *15*, 132–134.

(45) Ferrin, T. E.; Huang, C. C.; Jarvis, L. E.; Langridge, R. *UCSF MidasPlus User's Manual*; University of California: San Francisco, 1989.